Journal of Chromatography, 484 (1989) 409–423
Elsevier Science Publishers B.V., Amsterdam — Printed in The Netherlands

CHROM. 21 891

PREPARATIVE HIGH-PERFORMANCE LIQUID CHROMATOGRAPHY UNDER GRADIENT CONDITIONS

I. BAND BROADENING IN GRADIENT ELUTION AS A FUNCTION OF SAMPLE SIZE

G. B. COX
Medical Products Department, E. I. du Pont de Nemours Inc., Glasgow, DE 19701 (U.S.A.)
and
L. R. SNYDER* and J. W. DOLAN
LC Resources Inc., 3182C Old Tunnel Road, Lafayette, CA 94549 (U.S.A.)

SUMMARY

Previous studies of gradient elution under mass-overload conditions are continued. Use of the Craig distribution model shows that there is a simple relationship between bandwidth, sample size and gradient conditions for single-solute samples. This allows the use of two or three experimental measurements to determine the saturation capacity of a column by a given sample. Several (reversed-phase) experimental studies with small-molecule samples provide quantitative confirmation of this model.

For the case of protein samples the model works equally well, but it appears that only 20–44% of the column capacity (as measured by saturation uptake) is available under separation conditions. The column capacity for lysozyme was measured as a function of pore diameter and the accessibility of the surface under separation conditions was found to increase with increasing pore size.

INTRODUCTION

It has been shown for the case of analytical (small-sample) separations that isocratic and gradient elution can be related in a straightforward fashion[1,2]; that is, well known relationships developed for isocratic high-performance liquid chromatography (HPLC) can be applied to "corresponding" gradient separations. This simple picture of gradient elution has since been extended[3–5] to include mass-overloaded separation. For "corresponding" separations (*i.e.*, similar conditions) of a mixture of two xanthines[3], it was shown that the same separation (resolution) resulted with either isocratic or gradient elution, as long as sample size was the same in the two runs being compared.

Computer simulations based on the Craig distribution process were also used to study band broadening in gradient elution as a function of sample size and gradient

0021-9673/89/$03.50

steepness[4]; however, some puzzling differences between isocratic and gradient separation were observed. In addition, experimental studies on band broadening *vs.* sample size and gradient conditions were reported for several protein samples[5]. Significant differences between observed and predicted results were found and attributed (incorrectly, as will be seen) to non-Langmuir sorption.

This paper describes additional work aimed at a better understanding of gradient elution separation under touching-band conditions. In Part II[6] these findings are applied to the design of a computer-simulation program for facilitating method development for the touching-band separation of peptide and protein samples by means of reversed-phase gradient elution.

THEORY

For the case of isocratic separation[7,8], it has been shown that band broadening in single-band separations can be described by

$$W^2 = W_o^2 + W_{th}^2 \tag{1}$$

where W is the baseline width of a mass-overloaded band, W_o is the corresponding width of a small-sample band and W_{th} is the contribution to band broadening from a large sample. Values of W_o and W_{th} can be expressed further as

$$\text{(isocratic)} \quad W_o = (16/N_o)^{\frac{1}{2}} t_o(1+k_o) \tag{2}$$

and

$$\text{(isocratic)} \quad W_{th} = (6)^{\frac{1}{2}} t_o k_o (w/w_s)^{\frac{1}{2}} \tag{3}$$

(see Appendix). Here, the various terms have their usual meaning; see the list of symbols at the end of this paper.

Corresponding expressions for W_o and W_{th} hav been derived for gradient elution[4]. However, these relationships are complex, and they exhibit only partial agreement with Craig simulations and experimental data (for small molecules) to be reported here. If we assume that the isocratic–gradient analogy holds, however, it is straightforward to derive (new) corresponding expressions for eqns. 2 and 3. In eqn. 2, the isocratic parameter k_o can be replaced by the k' value at elution in gradient elution[1,2]:

$$k_e = 1/2.3b \tag{4}$$

where

$$b = V_m \Delta\varphi S/t_G F \tag{5}$$

The parameter b measures the steepness of the gradient, t_G is gradient time, F is flow-rate, V_m is column dead volume, $\Delta\varphi$ is the change in the volume fraction, φ, of

organic solvent during the gradient ($\Delta\%B/100$) and S is an isocratic property of the solute:

$$S = \mathrm{d}(\log k')/\mathrm{d}\varphi$$

$$\approx 0.48M^{0.44} \tag{6}$$

where M is the molecular weight of the solute.

Replacing k_o in eqn. 2 by k_e from eqn. 4 then gives

$$\text{(gradient)} \quad W_o = (16/N_o)^{\frac{1}{2}} t_o GJ[1+(1/2.3\ b)] \tag{7}$$

The factor G is included to account for the compression of the band by the gradient[1]. The factor J ($1 < J < 1.8$) represents an anomalous band broadening as b increases[a]; for Craig simulations, J can be assumed to be equal to 1. In most prepatative separations, a small-scale separation will be carried out initially, so that values of W_o will be known or calculable.

A similar substitution of k_e for k_o in eqn. 3 gives[b]

$$\text{(gradient)} \quad W_{th} = (6)^{\frac{1}{2}}\ t_o k_e G(w/w_s)^{\frac{1}{2}}$$

$$= 1.06 t_o G(w/w_s)^{\frac{1}{2}}/b \tag{8}$$

The mass-related band broadening, W_{th}, is of primary concern here. Previously it had been suggested[4,5] that W_{th} can be approximated by an expression of the form

$$W_{th} \approx \text{constant} \cdot (t_o/b)w^z \tag{9}$$

where $z \approx 0.85$ for a Langmuir isotherm (Craig simulations).

Experimental data for proteins showed good agreement with eqn. 9, except that $0.4 < z < 0.6$. In this paper it will be argued that Langmuir sorption should actually result in $z \approx 0.5$–0.6, suggesting that data previously reported[5] for the mass-overload gradient separation of proteins are in agreement with eqn. 8, and by inference those samples exhibit Langmuir sorption.

EXPERIMENTAL

Instrumentation

Chromatography was performed using either (1) a Hewlett-Packard (Avondale, PA, U.S.A.) 1090 liquid chromatograph fitted with a preparative injection accessory, (2) a DuPont (Wilmington, DE, U.S.A.) 8800 LC system using a Rheodyne septumless injection valve (fitted with a variety of loop sizes) plus a DuPont spectrophotometer

---

[a] In experimental systems, the product $JG \approx 1.1$ for different values of b. This simplifies the estimation of values of W_o as a function of gradient conditions.

[b] It is not yet known whether the effect represented by J for experimental small-sample separations (W_o, eqn. 7) will also apply to W_{th}; we assume not, until data to the contrary are reported.

TABLE I

PHYSICAL PROPERTIES AND SATURATION CAPACITIES OF DIFFERENT COLUMN PACKINGS WITH LYSOZYME SOLUTE

Packing[a]	*Pore diameter (nm)*	*Surface area (m^2/g)*	w_s[b] *(mg)*	w_s/SA[c] *(mg/m^2)*
C_8	7	300	70	0.13
PRO-10 C_8	13	160	112	0.39
PSM 120 C_8	12	98	70	0.39
PSM 300 C_8	30	50	50	0.55
PSM 500 C_8	50	30	34	0.63
PSM 1000 C_8	100	20	25	0.69

[a] Zorbax.
[b] Determined by breakthrough method.
[c] Column capacity w_s divided by column surface area SA; column contains 1.8 g of packing.

detector (fitted with a preparative flow cell) or (3) an LKB (Gaithersburg, MD, U.S.A.) gradient system using a DuPont spectrophotometer detector.

Columns

All columns were stainless steel (15 × 0.46 cm I.D.) and were loaded by a downward high-pressure slurry technique. The packing materials used are shown in Table I, together with their pore sizes, surface areas and particle sizes. All were Zorbax PSM silica (DuPont) which had been bonded with octadecyldimethylchlorosilane and capped with trimethylchlorosilane (Petrarch, Bristol, PA, U.S.A.) by conventional bonding techniques similar to those described by Kinkel and Unger[9].

Chemicals and protein standards

Solvents were of HPLC grade (J. T. Baker, Phillipsburg, NJ, U.S.A.) and were degassed with helium during use. Trifluoroacetic acid and sodium dihydrogen phosphate were of Baker Analyzed grade.

Protein standards were obtained from Sigma (St. Louis, MO, U.S.A.). All chemicals and standards were used without further purification.

Craig simulations

The model and software used in the present Craig simulations (CRAIG4) are similar to those reported earlier[4,10] and are described in detail in ref. 11. CRAIG4 was written for rapid calculations on an IBM-AT personal computer. Separations involving 1000–2000 plates can be carried out in 0.5–4 h running time, in either an isocratic or gradient mode, and for either one-component or two-component samples.

Verification of the present Craig simulations. The CRAIG4 program was used to calculate retention times and bandwidths for several small-sample isocratic and gradient elution separations, which can be compared with exact calculations as in ref. 4; all such comparisons showed excellent agreement (within a few tenths of a per cent for retention, within a few per cent for bandwidth). Similar comparisons were made for isocratic 1-solute mass-overloaded runs between previously reported computer-simulation results[12] and the same simulations via CRAIG4. These showed good

agreement (Fig. 1), confirming at least the consistency of the present approach. Comparisons in this paper of Craig with experimental gradient separations provide additional verification of the CRAIG4 software.

RESULTS AND DISCUSSION

Craig simulations

Isocratic data. In an effort to resolve certain anomalies in our previous Craig simulation treatment of mass-overloaded gradient elution[4,5] ($z \approx 0.85$ in eqn. 9), we first examined the case of isocratic separation; see also the discussion in ref. 11. Some representative data are shown in Fig. 1 for the sample-mass contribution to band broadening (W_{th}) as a function of sample size. The open points are from a previous study[a] and the closed triangles are new data from the use of CRAIG4. Three different data sets are plotted, for different values of k_0. The solid curves for these data points are a best fit to eqn. 3, assuming a single value of w_s for these simulations. For sample sizes $w/w_s > 0.1$, these initially linear plots are seen to curve downwards, as is predicted for heavily overloaded separations[4,7,13,14].

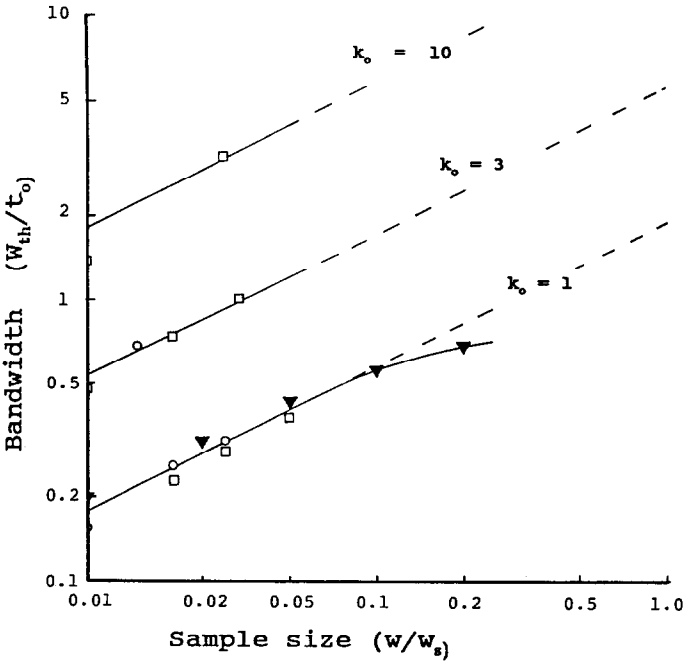

Fig. 1. Craig simulations of band broadening in isocratic separation as a function of sample size (cf., eqn. 3). Straight-line plots through these data are a best fit to eqn. 3 (see text). □, ○ = Data from ref. 12 for n_c = 600 and 1000, respectively; ▼ = data using CRAIG4.

[a] The open points in Fig. 1 are from ref. 12. The isotherm algorithms (polynomial fit) used in that study (for a single solute, fixed values of k_0 and small values of w/w_s) are presumed to be slightly more accurate than the corresponding algorithms[12] of CRAIG4.

For moderate overloading of the column ($w/w_s < 0.10$), we have shown previously that values of W_{th} appear to increase more rapidly than predicted by theory[13] or Craig simulation[11,15]. That is, the sample sizes used in Craig simulation give W_{th} values that are too small. This can be corrected by increasing the sample sizes used in Craig simulation 1.8-fold[11], in which case Craig and experimental predictions of bandwidth are brought into agreement.

The data in Fig. 1 when fitted to eqn. 3 can be used to verify this correction factor (1.8-fold) for Craig simulation *vs.* the case of experimental data. This yields a value of 2.1-fold, which is reasonably close to the the above factor of 1.8. That is, any conclusions we obtain from isocratic Craig simulation must be modified for application to experimental separations; the value of w/w_s assumed in Craig simulations should be about 1.8-fold higher than for corresponding experimental systems if good agreement between experimental and Craig simulation results is to be obtained.

Gradient elution. Eqns. 8 and 9. Fig. 2 illustrates some CRAIG4 simulations for a single band as a function of sample size (other conditions remaining the same). A similar pattern was observed[4] in previous Craig simulations of gradient elution: overlapping ("nested") bands having a "shark-fin" shape. Values of W_{th} can be obtained for these various bands (eqn. 1); Fig. 3 shows a log–log plot of W_{th} *vs* sample size (w/w_s).

The data in Fig. 3 lie on a straight line, in agreement with eqn. 9. The slope of this straight-line plot is $z = 0.6$, in contrast to previous studies[4] which gave $z = 0.85$. There are several reasons for this difference between the present and previous Craig-

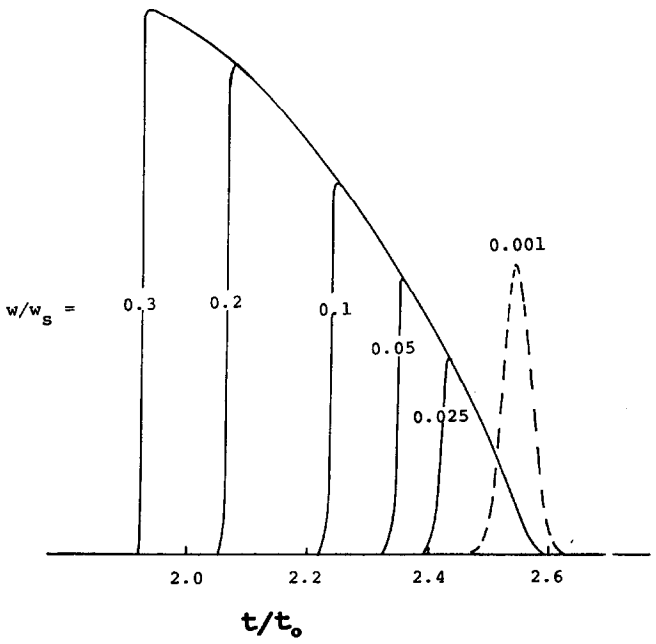

Fig. 2. Craig simulations (CRAIG4) for the gradient elution separation of a single band as a function of sample size. Conditions: $N_o = 1600$ ($n_c = 800$), $b = 1$, k_o at the start of the gradient (k_{og}) = 10.

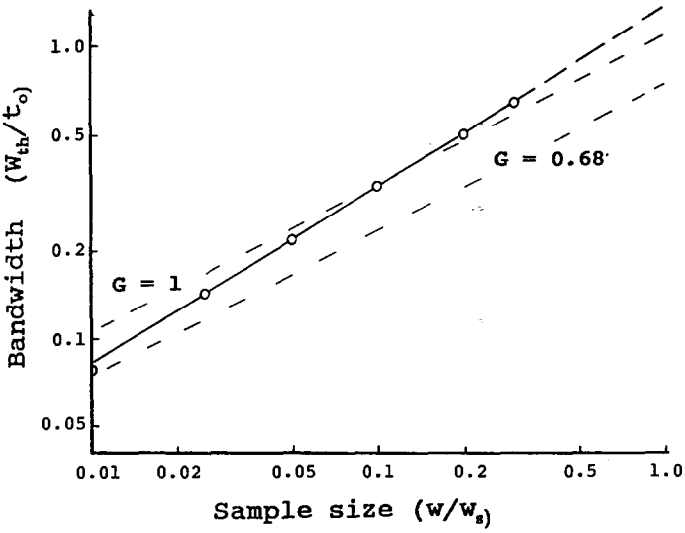

Fig. 3. Craig simulations of band broadening in gradient separation as a function of sample size (cf., eqn. 8). Dashed straight-line plots are predicted by eqn. 8 for different values of G (see tect). Data points (○) correspond to separations in Fig. 2 (same conditions).

simulation studies. First, we now know that the way in which bandwidths are measured for mass-overloaded bands can significantly affect values of W_{th} when w/w_s is small. It is relatively easy to determine the beginning of the band by the tangent method (see the examples in Fig. 2), but the end of the band is often ambiguous. We now feel that the best approximation to the end of the band is given by $t_R^0 + (w_o/2)$, where t_R^0 is the small-sample retention time. Second, Craig simulations are more reliable for larger values of N_o (larger values of n_c, the number of Craig stages)[12]. The data in Fig. 3 ($n_c = 800$) are based on twice the number of plates used in our previous study[4]. Finally, the algorithms used in CRAIG4 were more thoroughly tested than in the previous study[4], and may therefore be more reliable.

The dashed curves in Fig. 3 are from eqn. 8, assuming either the value of G for a small-sample separation ($G = 0.68$) or negligible band compression by the gradient ($G = 1$). For small samples ($w/w_s < 0.01$), there is no reason to believe that gradient compression should not affect the entire band (values of both W_o and W_{th}). For larger samples, however, the front of the band moves in a mobile phase that is much weaker (larger k_0). This corresponds to a smaller value of b (eqn. 4), for which the value of G then approaches 1, *i.e.*, there is negligible gradient compression for a small-sample band as the gradient becomes flatter (and approaches isocratic separation[a]). We therefore expect that plots as in Fig. 3 will approach the curve predicted by eqn. 8 ($G = 0.68$ in this case, for $b = 1$) for smaller samples, then trend toward the corresponding curve for $G = 1$ with larger samples. This is observed for the example in Fig. 3.

[a] This effect applies only to the front of the band, which is traveling through the column in a much weaker solvent. Therefore, the lack of gradient compression at the band front does not have much effect on the "shark fin" shape of the band (see Fig. 2).

In addition to demonstrating the agreement of eqn. 8 with these Craig simulations[a], Fig. 3 also shows that values of z should vary between roughly 0.5 and 0.6. For smaller values of b ($b = 1$ in Fig. 3), corresponding to more common gradient conditions, the lower dashed curve in Fig. 3 will approach the upper curve, so that then $z \approx 0.5$. For steeper gradients as in Fig. 3, z will tend toward a value of about 0.6. We shall see that this corresponds fairly well to experimental gradient elution separations.

EXPERIMENTAL

Small solute molecules

Two small-molecule solutes, caffeine and benzyl alcohol, were chosen for an experimental study of bandwidth *vs.* sample size in reversed-phase gradient elution. Previous studies[15] have shown that these solutes exhibit Langmuir-isotherm behaviour under reversed-phase conditions.

Caffeine as solute. Chromatography for caffeine was performed on a 15 × 0.46 cm I.D. column packed with Zorbax PSM 500 C8 (500 Å pore diameter, 8 μm particle size) with methanol and 0.05 M sodium phosphate (pH 5) as mobile phase components. This large-pore silica was chosen because its low surface area (and small value of w_s) allow the observation of mass-related band broadening for reasonably small samples, thus avoiding problems with sample solubility.

As we intended to compare our findings with the theoretical predictions of eqn. 8, values of the gradient-steepness parameter b were required. This in turn requires a value for the solute parameter S (eqn. 5). Exact values of S for a particular solute and HPLC system can be obtained using either isocratic or gradient data. For isocratic retention,

$$\log k_0 = \log k_w - S\varphi \tag{10}$$

Therefore, measurement of values of k' as a function of mobile phase composition φ serve to determine a value of S. Alternatively, two gradient runs with different values of b (different gradient steepness) can also be used[16]. For the HPLC system in Table II, values of S and k_w for caffeine were $S = 8.2$ (isocratic) and 7.9 (gradient) and $k_w = 26.0$ (isocratic) and 25.7 (gradient). Average values of $S = 8.0$ and $k_w = 25.8$ were assumed in further work.

The saturation capacity of the column for caffeine was next determined as described earlier[8] (based on eqns. 2 and 3 in ref. 11). Isocratic chromatograms were obtained using methanol–0.05 M sodium phosphate (10:90) as the mobile phase for a low (0.01 mg) and a high (0.1 mg) load of caffeine. Calculation of the saturation capacity (w_s) gave a value of 20 mg (equal to 0.33 mg/m^2 for this packing).

Gradient elution with sample sizes from 0.01 to 10.0 mg of caffeine were carried out under two sets of gradient conditions (corresponding to $b = 0.33$ and 0.165), *i.e.*, gradients from 0 to 50% B in 30 or 60 min (A is 0.05 M phosphate, B is methanol). Bandwidths W were measured, and mass-related bandwidths W_{th} were calculated for

[a] Note that the Craig simulations in Fig. 3 are uncorrected for the 1.8-fold discrepancy found in ref. 11; that is, these Craig simulations for gradient elution are in much closer agreement with theory as expressed by eqn. 8. The reason for this difference between isocratic and gradient separations is not yet clear.

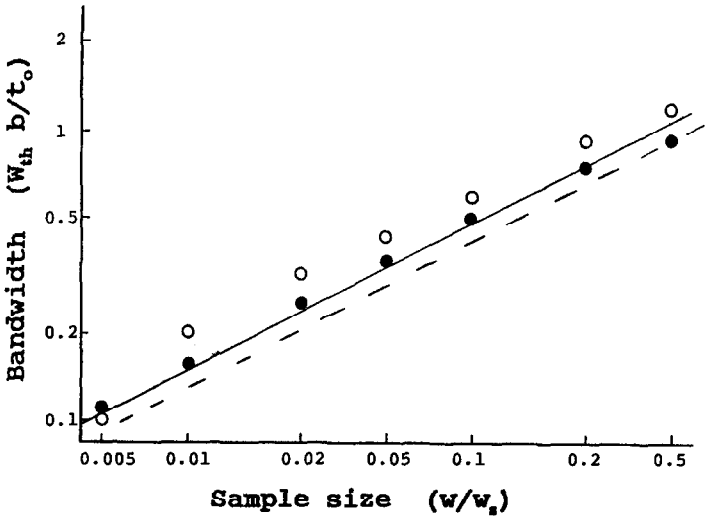

Fig. 4. Sample size-dependent band broadening for gradient elution runs with caffeine as solute. Conditions: 15 × 0.46 cm I.D. Zorbax PSM 500 C_8 column; 0–50% B gradient (A, 0.05 *M* sodium phosphate, pH 5; B, methanol); 1 ml/min. ○ = Gradient time 30 min; ● = gradient time 60 min. Solid line, $G = 1$; dashed line, $G = 0.85$.

each gradient run from eqn. 1 (using an experimental value of W_0). Fig. 4 shows resulting plots of $W_{th}b/t_0$ *vs.* w/w_s for both gradient conditions. The solid line is from eqn. 8, with $G = 1$, and the dashed line is for the small-sample G value of 0.85. The agreement between the experimental and calculated values is fairly good, although the bandwidths for the steeper gradient are slightly higher than expected. If the data of Fig. 4 are fitted to eqn. 9, a best value of $z = 0.46$ is obtained.

Benzyl alcohol as solute. Chromatography for benzyl alcohol was performed on a 15 × 0.46 cm I.D. Zorbax ODS column with methanol–water mixtures as the mobile phase. Values of S and k_w for this solute were determined as above: $S = 2.4$ (isocratic) and 2.2 (gradient) and $k_w = 32$ (isocratic) and 25 (gradient). Average values of these parameters were assumed in further work. The value of w_s for this packing and benzyl alcohol as solute was reported in ref. 15 as 64 mg for a 5-cm column; we have assumed $w_s = 192$ mg for the present 15-cm column. Fig. 5 shows a plot of W_{th} *vs.* w/w_s in the same manner as in Fig. 4 for caffeine. The best fit of these data to eqn. 9 gives $z = 0.54$. Again, there is reasonable agreement between observed and predicted results.

3-Hydroxypropyltheophylline (HPT) as solute. The gradient separation of this xanthine in admixture with hydroxyethyltheophylline (HET) has been reported[3] as a function of sample size. Plots of W_{th} *vs.* sample size can be derived, as in Figs. 4 and 5. These data are plotted in Fig. 6. The comparison of experimental values (○) with calculated curves (dashed lines) as in Figs. 4 and 5 gives a similar result, although the experimental values are now slightly lower than predicted. In this instance, the data for HTP may be affected by the presence of HET in the sample (the experiments in Figs. 4 and 5 involved single-solute samples). The value of z is 0.61.

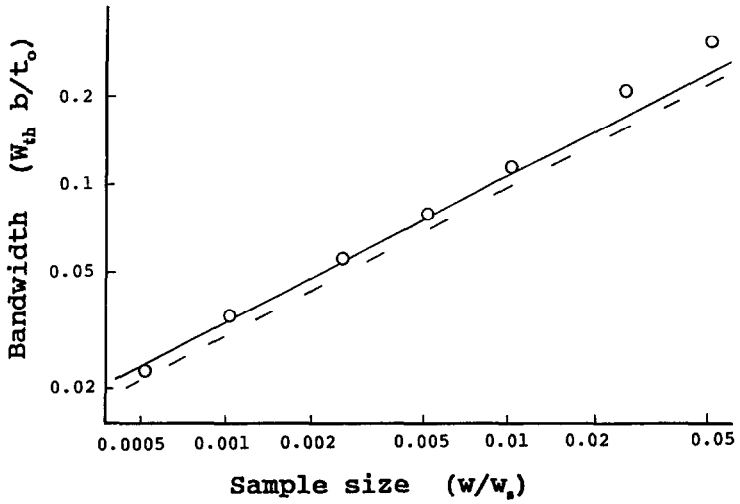

Fig. 5. Sample size-dependent band broadening for gradient elution runs with benzyl alcohol as solute. Conditions: 15 × 0.46 cm I.D. Zorbax ODS column; 0–50% methanol–water gradient in 30 min; 1 ml/min. Solid line, $G = 1$; dashed line, $G = 0.90$.

Protein solutes

Twelve plots of W_{th} *vs.* w (similar to those in Figs. 4–6) for various proteins and different reversed-phase columns were reported previously[5]. The observed value of z for all systems was found to be 0.54 ± 0.08 (S.D.), which is in good agreement with eqn. 8 and the discussion in Fig. 4. Therefore the conclusion in ref. 4 that reversed-phase protein separations appear not to follow Langmuir adsorption (which

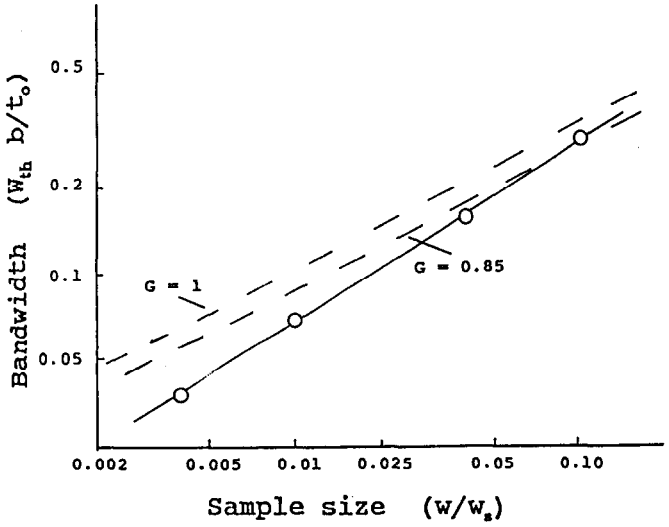

Fig. 6. Sample size-dependent band broadening for gradient elution runs with 3-hydroxypropyltheophylline as solute. Conditions: 15 × 0.46 cm I.D. Zorbax C_8 column; 5–100% B in 14.8 min [A = 0.1 *M* phosphate, pH = 2.2; B = acetonitrile–methanol (20:80, v/v)]; 1 ml/min. Solid line, $G = 1$; dashed line, $G = 0.85$.

is implicit in the derivation of eqn. 8) is incorrect. These HPLC systems may in fact exhibit non-Langmuir behavior in other respects, but the dependence of W_{th} on sample size (value of z) is consistent with Langmuir adsorption.

Column capacity w_s for protein samples as a function of column-packing pore diameter. The possibility that Langmuir adsorption is able to explain the separation of proteins as solutes for reversed-phase gradient elution can be tested further by making independent measurements of the column capacity, w_s (w_s values were not determined in the studies in ref. 5). The column capacity for a protein sample can be measured in various ways. We used successive injections of small amounts of protein with a weak mobile phase[a] until breakthrough is observed. The retained protein can then be eluted in a gradient run, as a check on the amount taken up. This approach was tried with lysozyme as a test solute and a 15 × 0.46 cm I.D. PSM 300 C_8 column. Within the limits imposed by the linearity of detector response (*i.e.*, high lysozyme concentrations plus a varying mobile phase composition), the amount of eluted protein (52 mg) agreed well with the amount measured in the breakthrough experiment (47 mg).

The column capacity of lysozyme was determined for a number of (otherwise identical) columns filled with packings of different pore size and surface areas. The results are given in Table I. As the pore diameter is increased from 7 to 100 nm, the column capacity first increases to a maximum of 112 mg for the packing of 13-nm pore diameter, then decreases continuously with further increase in pore diameter. Further insight into these column-capacity data are afforded by the surface areas (Table I) and column capacities per square meter of surface (last column of Table I).

In general, the surface area (m^2/g) of a packing decreases as the pore diameter increases. However, large solute molecules do not have access to all the pores of the packing, because of possible steric exclusion. Therefore, for a protein of intermediate size (lysozyme in the present example) the column capacity per square meter will increase with increasing pore diameter, but eventually approach a limiting value (about 0.7 mg/m^2) for the data in Table I. The latter dependence, combined with a continuous decrease in surface area with increasing pore diameter, then results in a maximum column capacity (for columns of given size, as in Table I) for an intermediate pore diameter (10–15 nm for lysozyme and reversed-phase columns). A similar situation has been described by Rounds *et al.*[17] for the ion-exchange separation of different proteins.

Column capacities inferred from eqn. 8. We have previously reported[5] values of W_{th} *vs.* sample size for the gradient elution separation of lysozyme and carbonic anhydrase, using columns similar to those in Table I. Eqn. 8 can be used to infer values of w_s for these various systems, for comparison with the saturation uptake values in Table I. The results are summarized in Table II.

It is seen that the w_s values from eqn. 8 are generally lower than the saturation-uptake values in Table II. Further, the fractional utilization of the total surface (as measured by saturation uptake) increases with increasing pore diameter. This suggests that under actual separation conditions (gradient elution as in ref. 5), protein samples can utilize only a fraction of the total surface available to the sample at

[a] We recommend 5–10% acetonitrile in water, rather than water alone, to allow adequate wetting of the packing by the mobile phase and avoid incomplete uptake of protein.

TABLE II

DYNAMIC COLUMN CAPACITIES INFERRED FROM DATA IN REF. 5 BY MEANS OF EQN. 8

Lysozyme solute, 15 × 0.46 cm I.D., 5-μm C_8 columns, 5–70% acetonitrile in 0.1%TFA–water gradients in 20 min, 1 ml/min.

Pore diameter of packing (nm)	w_s *(mg)*		*% surface utilization*[c]
	Table I[a]	*Eqn. 8*[b]	
15	80[d]	18	23
30	50	10	20
50	34	10	29
100	25	11	44

[a] Data from Table I except where noted otherwise.
[b] Eqn. 8 applied to data in ref. 5 (Figs. 8–11 in that paper).
[c] Eqn. 8 values divided by Table I values.
[d] Different packing to that shown in Table I; interpolated value from plot of w_s *vs.* pore diameter.

equilibrium. This fractional utilization apparently increases with more facile mass transfer (larger pores), as suggested also by the work of Kopaciewicz *et al.*[18].

The data in Table II suggest that actual column capacities (which determine the column loadability in gradient elution) for protein samples vary with column pore diameter in a complex fashion. This has obvious practical implications, which we will explore further elsewhere. Returning to the question of whether protein samples obey the Langmuir isotherm, it should be obvious that no final conclusions regarding this point can be drawn from the present study. The fact that the apparent column capacity for protein samples (in gradient elution) is less than the saturation uptake value suggests that both equilibrium (isotherm) and kinetic (mass transfer) effects contribute to the dependence of W_{th} on sample size. Under these circumstances, the observed agreement between Eqn. 8 and experimental data for proteins could be fortuitous.

Velayudhan and Horváth[19] argued against a Langmuir isotherm for the ion-exchange separation of proteins, in view of the fact that a single protein molecule will displace several salt ions (the Langmuir equation assumes a one-to-one displacement process). Similar logic can be used against a Langmuir isotherm for protein samples in reversed-phase systems, because of the evidence that reversed-phase retention also involves a displacement process[20]. Previously we have considered[15] the consequences of a non-stoichiometric displacement process as this affects Langmuir-type sorption processes. An extension of that treatment suggests that the sorption of protein molecules, with the resulting displacement of many solvent molecules by each sorbing protein molecule, can be approximated fairly well by the Langmuir equation (for $w/w_s < 0.5$), if the actual column capacity w_s is reduced by about half. This observation is suggestive in the light of the data in Table II, *i.e.*, the percentage surface utilization values shown there should actually be doubled.

CONCLUSIONS

The dependence of band broadening and separation in gradient elution has been further studied by both theoretical and experimental means. For the case of small

molecules, bandwidth as a function of sample size and gradient conditions can be described by a simple equation (eqn. 8). This relationship predicts that the mass-related contribution to bandwidth (W_{th}) will be proportional to (sample weight)^z, where z will normally vary between 0.5 and 0.6. Computer simulations based on the Craig distribution process confirm this relationship. Experimental data for several small-molecule samples are also in quantitative agreement with eqn. 8. It therefore appears that we have a reasonably good understanding of band broadening for a one-component sample as a function of sample size and separation conditions.

The gradient elution separation of protein samples by reversed-phase HPLC appears more complex. The same general relationship (eqn. 8 with $0.5 < z < 0.6$) also describes band broadening *vs.* sample size for these samples, but the apparent column capacities (w_s) inferred from band-broadening data are generally smaller than values measured by saturation uptake. This suggests that the mass-related contribution to band broadening (W_{th}) is a function of both equilibrium and kinetic properties of the system, unlike the case for small-molecule solutes. Nevertheless, a broad range of protein systems have been shown to exhibit a predictable increase in bandwidth with increasing sample size, as discussed further in Part II.

APPENDIX

Derivation of eqn. 3

This relationship has been reported previously[8] but not actually derived. We start with previous expressions for experimental values of N (for a large sample) and N_o (see ref. 11):

$$N_o = 16(t_R^o/W_o)^2 \tag{A1}$$

$$N = 16(t_R^o/W)^2 \tag{A1a}$$

$$N/N_o = 1/[1 + (3/8)w_{xn}] \tag{A2}^a$$

$$w_{xn} = N_o[k_o/(1+k_o)]^2(w/w_s) \tag{A3}$$

$$t_R^o = t_o(1+k_o) \tag{A4}$$

Eqns. 1, A2 and A4 combine to give

$$1/N = (w_o^2 + W_{th}^2)/16[t_o(1+k_o)]^2 \tag{A5}$$

Likewise, eqn. A2 can be written as

$$1/N = 1/N_o + [(3/8)w_{xn}/N_o] \tag{A6}$$

---

[a] This equation[7] is a best fit to experimental values of N; the corresponding *theoretical* expression[7,13] is $N/N_o = 1/[1+(1/4)w_{xn})]$, which leads to the replacement of the factor $(6)^{\frac{1}{2}}$ in eqn. 3 by the factor 2.

Eqns. 1, A1 and A1a give

$$(1/N) - (1/N_o) = (W^2/16t_R^{o2}) - (W_o^2/16t_R^{o2})$$

$$= W_{th}^2/16t_R^2 \quad \text{(A7)}$$

Eqn. A6 can be rewritten as

$$(1/N) - (1/N_o) = (3/8)w_{xn}/N_o \quad \text{(A8)}$$

Eqns. A7 and A8 then give

$$W_{th}^2/16t_R^2 = (3/8)w_{xn}/N_o \quad \text{(A9)}$$

Eqns. A3, A4 and A9 then give eqn. 3.

SYMBOLS (PARTS I–III)

Reference to equations or figures in the various papers in this series is identified by use of I-, II- or III-, *e.g.*, eqn. III-3 refers to eqn. 3 in Part III.

b	gradient steepness parameter; equal to $[1/(1.15\bar{k})]$ (eqn. I-5)
B	strong solvent in the mobile phase
F	flow-rate (ml/min)
G	gradient compression factor (eqn. I-7)
J	anomalous band-broadening factor in gradient elution (eqn. I-7)
k'	solute capacity factor
$\bar{k}$	average value of k' during gradient elution; equal to $[1/(1.15b)]$
k_e	value of k' in gradient elution when the band leaves the column (eqn. I-4)
k_o	value of k' for a small sample
k_w	value of k' for water as mobile phase
k_{wx}, k_{wy}	values of k_w for X and Y
M	solute molecular weight
n_c	number of Craig stages in a computer simulation; $n_c = [k'/(1+k')]N_o$
N_o	value of N for a small sample; in computer simulations, $N_o = [(1+k')/k']n_c$
P_R	production rate; mg/h of purified product
R_s	resolution
R_s'	value of R_s in an initial run (eqn. II-6)
$R_{s\ opt}$	optimum value of R_s (in a small-sample separation) to maximize resolution in a preparative run (eqn. II-6)
S	parameter that measures change in isocratic k' values with change in φ (eqn. 6)
SA	stationary phase surface area (m^2 for entire column)
S_x, S_y	values of S for X and Y
t_D	dwell time of gradient equipment (min)
t_g	retention time in gradient elution (min)
t_G	gradient time (min)
t_o	column dead time (min)

t_x, t_y	retention times in gradient elution for bands X and Y (min, small sample)
V_m	column dead volume (ml)
w	total weight of injected sample; usually combined weights of X and Y (mg)
W	baseline bandwidth (min); see Figs. 2 and 3
W_o	value of W for a small sample (min) (eqn. I-1)
w_s	column saturation capacity (mg)
W_{th}	sample-size contibution to W (min) (eqn. I-1)
w_x, w_y	weight of solutes X or Y injected on the column (mg)
x,y	subscripts referring to bands X and Y
X, Y	adjacent sample bands; Y corresponds to the desired product and X is the preceding band
z	slope of plot of W_{th} *vs.* w (I-9)
α	separation factor for two solutes
$\Delta\varphi$	change in φ during a gradient
φ	mobile phase composition; volume fraction of strong solvent B in the mobile phase
φ_i, φ_f	initial (i) and final (f) values of φ in a gradient

REFERENCES

1 L. R. Snyder, in Cs. Horváth (Editor), *High-Performance Liquid Chromatography —Advances and Perspectives*, Vol. 1, Academic Press, New York, 1986, p. 207.
2 L. R. Snyder and M. A. Stadalius, in Cs. Horváth (Editor), *High-Performance Liquid Chromatography —Advances and Perspectives*, Vol. 4, Academic Press, New York, 1986, p. 195.
3 J. E. Eble, R. L. Grob, P. E. Antle and L. R. Snyder, *J. Chromatogr.*, 405 (1987) 51.
4 L. R. Snyder, G. B. Cox and P. E. Antle, *J. Chromatogr.*, 444 (1988) 303.
5 G. B. Cox, P. E. Antle and L. R. Snyder, *J. Chromatogr.*, 444 (1988) 325.
6 L. R. Snyder, J. W. Dolan, D. C. Lommen and G. B. Cox, *J. Chromatogr.*, 484 (1989) 425.
7 L. R. Snyder, G. B. Cox and P. E. Antle, *Chromatographia*, 24 (1987) 82.
8 L. R. Snyder and G. B. Cox, *LC · GC, Mag. Liq. Gas Chromatogr.*, 6 (1988) 894.
9 J. N. Kinkel and K. K. Unger, *J. Chromatogr.*, 316 (1984) 193.
10 J. E. Eble, R. L. Grob, P. E. Antle and L. R. Snyder, *J. Chromatogr.*, 405 (1987) 1.
11 L. R. Snyder, J. W. Dolan and G. B. Cox, *J. Chromatogr.*, 483 (1989) 63.
12 J. E. Eble, R. L. Grob, P. E. Antle and L. R. Snyder, *J. Chromatogr.*, 384 (1987) 25.
13 J. H. Knox and H. M. Pyper, *J. Chromatogr.*, 363 (1986) 3.
14 S. Goshan-Shirazi and G. Guiochon, *Anal. Chem.*, 60 (1988) 2364.
15 J. E. Eble, R. L. Grob, P. E. Antle and L. R. Snyder, *J. Chromatogr.*, 384 (1987) 45.
16 M. A. Quarry, R. L. Grob and L. R. Snyder, *Anal. Chem.*, 58 (1986) 907.
17 M. A. Rounds, W. Kopaciewicz and F. E. Regnier, *J. Chromatogr.*, 362 (1986) 187.
18 W. Kopaciewicz, S. Fulton and S. Y. Lee, *J. Chromatogr.*, 409 (1987) 111.
19 A. Velayudhan and Cs. Horváth, *J. Chromatogr.*, 443 (1988) 13.
20 X. Geng and F. E. Regnier, *J. Chromatogr.*, 296 (1984) 15.